# A weakly structured stem for human origins in Africa

Aaron P. Ragsdale<sup>1</sup>, Timothy D. Weaver<sup>2</sup>, Elizabeth G. Atkinson<sup>3</sup>, Elieen Hoal<sup>4</sup>, Marlo Möller<sup>4</sup>, Brenna M. Henn<sup>2,5,†,\*</sup>, and Simon Gravel<sup>6,†,\*\*</sup>

<sup>1</sup>Department of Integrative Biology, University of Wisconsin–Madison, WI, USA
<sup>2</sup>Department of Anthropology, University of California, Davis, Davis, CA, USA
<sup>3</sup>Department of Molecular and Human Genetics, Baylor College of Medicine, Houston, TX, USA
<sup>4</sup>DSI-NRF Centre of Excellence for Biomedical Tuberculosis Research; South African Medical Research Council Centre for Tuberculosis Research; Division of Molecular Biology and Human Genetics, Faculty of Medicine and Health Sciences, Stellenbosch University, Cape Town, South Africa
<sup>5</sup>UC Davis Genome Center, University of California, Davis, Davis, CA, USA
<sup>6</sup>Department of Human Genetics, McGill University, Montreal, QC, Canada

<sup>†</sup>Co-Corresponding Authors

\*bmhenn@ucdavis.edu

\*\*simon.gravel@mcgill.ca

January 6, 2023

16 Abstract

While it is now broadly accepted that Homo sapiens originated within Africa, considerable uncertainty surrounds specific models of divergence and migration across the continent. Progress is hampered by a paucity of fossil and genomic data, as well as variability in prior divergence time estimates. Here we use linkage disequilibrium and diversity-based statistics, optimized for rapid, complex demographic inference to discriminate among such models. We infer detailed demographic models for populations across Africa, including representatives from eastern and western groups, as well as 44 newly whole-genome sequenced individuals from the Nama (Khoe-San). Despite the complexity of African population history, contemporary population structure dates back to Marine Isotope Stage (MIS) 5. The earliest population divergence among contemporary populations occurs 120-135ka, between the Khoe-San and other groups. Prior to the divergence of contemporary African groups, we infer long-lasting structure between two or more weakly differentiated ancestral Homo populations connected by gene flow over hundreds of thousands of years (i.e. a weakly structured stem). We find that weakly structured stem models provide more likely explanations of polymorphism that had previously been attributed to contributions from archaic hominins in Africa. In contrast to models with archaic introgression, we predict that fossil remains from coexisting ancestral populations should be morphologically similar. Despite genetic similarity between these populations, an inferred 1-4% of genetic differentiation among contemporary human populations can be attributed to genetic drift between stem populations. We show that model misspecification explains variation in previous divergence time estimates and argue that studying a suite of models is key to robust inferences about deep history.

## Introduction

10

11

12

13

14

15

17

18

19

20

21

22

23

24

25

26

27

28

29

30

31

32

33

34

35

Decades of study of human genome variation have suggested a predominantly tree-like model of recent population divergence from a single ancestral population in Africa. It has been difficult to reconcile this finding with the fossil and archaeological records of human occupation across the vast African continent. For example, fossils such as those from the sites of Jebel Irhoud, Morocco<sup>1</sup>, Herto, Ethiopia<sup>2</sup> and Klasies River, South Africa<sup>3</sup> demonstrate that derived *Homo sapiens* anatomical features were found across the continent 300-100ka. Archaeological sites from the Middle Stone Age, of which some have been associated with *Homo sapiens*, are also widely distributed across Africa. It is unclear whether these fossils and archaeological sites represent populations which contributed to contemporary *Homo sapiens* as population precedents or were

local "dead-ends". Recently, attempts to reconcile genetic and paleoanthropological data include proposals for a Pan-African origin of *Homo sapiens* by which populations in many regions of the continent contributed to the formation of *Homo sapiens* beginning at least 300ka <sup>4,5,6</sup>.

Genetic models have been hampered in their contribution to this discussion because they primarily assume (or, at least, have been tested under) a tree-like model of isolation-with-migration. Alternative theoretical scenarios have been proposed, such as stepping stone models<sup>7</sup> or population coalescence and fragmentation<sup>6</sup> but these approaches are more challenging to interpret and fit to data. However, new population genetic tools now allow for inference involving tens to hundreds of genomes from multiple populations and greater complexity<sup>8,9,10</sup>. Inspired by evidence for Neanderthal admixture with humans in Eurasia, several recent articles have shown that introducing an archaic hominin ghost population contributing to African populations in the period surrounding the Out-of-Africa migration event substantially improves the description of genetic data relative to single-origin models, mostly in Western Africa 11,12,13,9,14,15, but also in southern 12,14 and central African 16,12,14 populations. This has driven speculation about the geographic range of this ghost population, possible links to specific fossils, and the possibility of finding ancient DNA evidence e.g., <sup>16</sup>. However, these prior articles share two weaknesses. First, they only contrast a single-origin model with an archaic hominin admixture model, leaving out other plausible models <sup>17</sup> (Figure 1). Second, they focus on a small subset of African diversity, either because of small sample sizes (2-5 genomes) or because they rely on 1000 Genomes data which only recruited populations of recent West African or Bantu-speaking ancestry (Figure 2C). While ancient DNA from Eurasia has helped us understand early human history outside of Africa, there is no comparably ancient DNA to elucidate early history in Africa <sup>18</sup>.

We therefore aim to discriminate among a broader set of demographic models by studying the genomes of contemporary populations. We take as our starting point four classes of models (single population expansion, single population expansion with regional persistence, archaic hominin admixture, and multi-regional evolution, Figure 1), using 290 genomes of individuals from southern, eastern, and western Africa as well as Eurasia. By including geographically and genetically diverse populations across Africa, we infer demographic models that explain more features of genetic diversity in more populations than previously reported. These analyses confirm the inadequacy of tree-like models and provide an opportunity to directly evaluate a wide range of alternative models.

### $_{\scriptscriptstyle 3}$ Results

47

49

51

52

53

55

56

57

58

59

62

63

64

66

71

We inferred detailed demographic histories using 4x-8x whole-genome sequencing data for four diverse African populations, comprising the Nama (Khoe-San from South Africa, newly presented here), Mende (from Sierra 75 Leone, MSL from the Phase 3 1000 Genomes Project 19), Gumuz (recent descendants of a hunter-gatherer 76 group from Ethiopia<sup>20,21</sup>), and eastern African agriculturalists (Amhara and Oromo from Ethiopia<sup>20</sup>). The 77 Amhara and Oromo populations, despite speaking distinct Afro-Asiatic languages, are highly genetically 78 similar <sup>22,21</sup> and thus the two groups were combined for a larger sample size (Figure 2). We also included 79 the British (GBR) from the 1000 Genomes Project in our demographic models as a representative source 80 of back-to-Africa gene flow and recent colonial admixture in South Africa. Finally, we used a high-coverage ancient Neanderthal genome from Vindija Cave, Croatia<sup>23</sup> to account for gene flow from Neanderthals 82 into non-Africans and gauge the relative time depth of divergence, assuming Neanderthals diverged 550ka from a common stem. We computed one- and two-locus statistics whose expectation within and across 84 populations can be computed efficiently and that are well suited for both low- and high-coverage genomes 9,24. Using a maximum-likelihood inference framework, we then fit to these statistics a family of parameterized demographic models that involve population splits, size changes, continuous and variable migration rates, and punctuated admixture events, to learn about the nature of population structure over the past million years.

#### A Late Pleistocene common ancestry for contemporary humans

We began with a model of geographic expansion from a single ancestral, unstructured source followed by migration between populations, without allowing for contribution from an African archaic hominin lineage or population structure prior to the expansion (Figure 1A or Figure 1D). As expected  $^9$ , this first model was a poor fit to the data qualitatively (Figure S11) and quantitatively (log-likelihood (LL)  $\approx -189,400$ ,

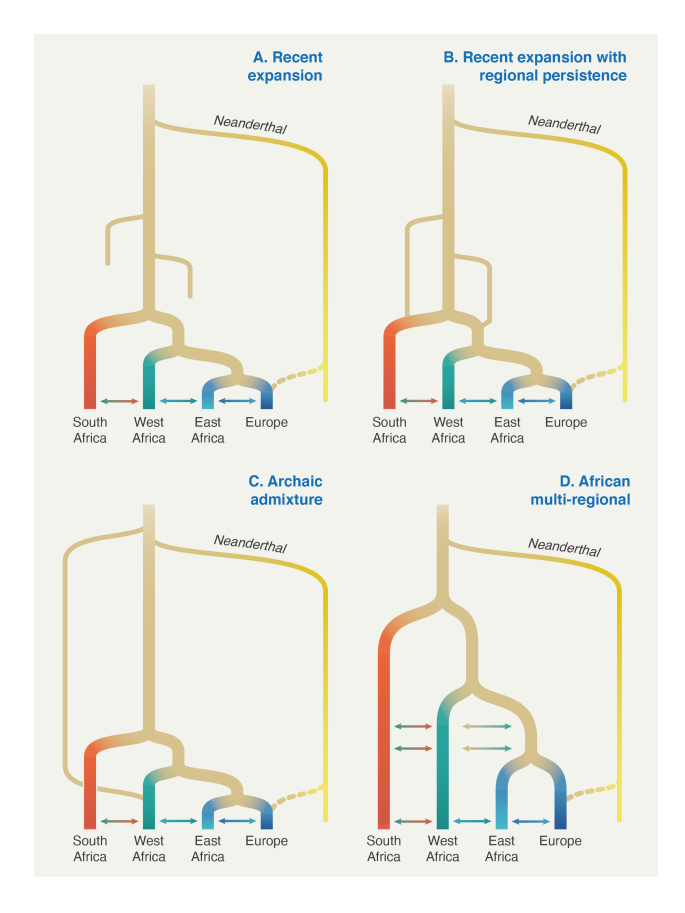


Figure 1: **Proposed conceptual models of early human history in Africa.** These models have been designed to translate models from the paleoanthropological literature into genetically testable demographic models <sup>17</sup>. We used these conceptual models as starting points to build detailed parameterized demographic models (SI Section 3) that were then fit to genetic data.

Table S3). We next explored a suite of parameterized models in which population structure predates the differentiation of contemporary groups (Supporting Information (SI) Section 3). Depending on the parameters, these encompassed models allowing for ancestral reticulation (such as fragmentation-and-coalescence or meta-population models, Figure 1B), archaic hominin admixture (Figure 1C), and African multi-regionalism (Figure 1D).

Regardless of the model choice for early epochs, maximum-likelihood inference of human demographic history for the last 150ka was remarkably robust. In a reticulated model, we use "divergence" between populations to mean the time of their most recent shared ancestry. The earliest divergence among contemporary human populations differentiates the southern African Nama from other African groups between 110–135ka, with low to moderate levels of subsequent gene flow (Table 1). In none of the high-likelihood models which we explored did the divergence between Nama and other populations exceed ~140ka. We conclude that geographic patterns of contemporary *Homo sapiens* population structure likely arise during MIS 5. Although we find evidence for earlier population structure in Africa (next section), contemporary populations cannot be easily mapped onto the more ancient 'stem' groups as only a small proportion of drift between contemporary populations can be attributed to drift between stems (SI Section 5.2, Figures 4 and S17–S20).

Given this consistency in inferred recent history and the numerical challenge of optimizing a large number of parameters, we fixed several parameters related to recent population history so as to focus on more ancient events. These parameters were ones supported by multiple genetic and archaeological studies. Fixed parameters included the time of divergence between western and eastern African populations, set to 60ka, just prior to the split of Eurasians and East Africans set to 50ka. We also fixed the amount of admixture

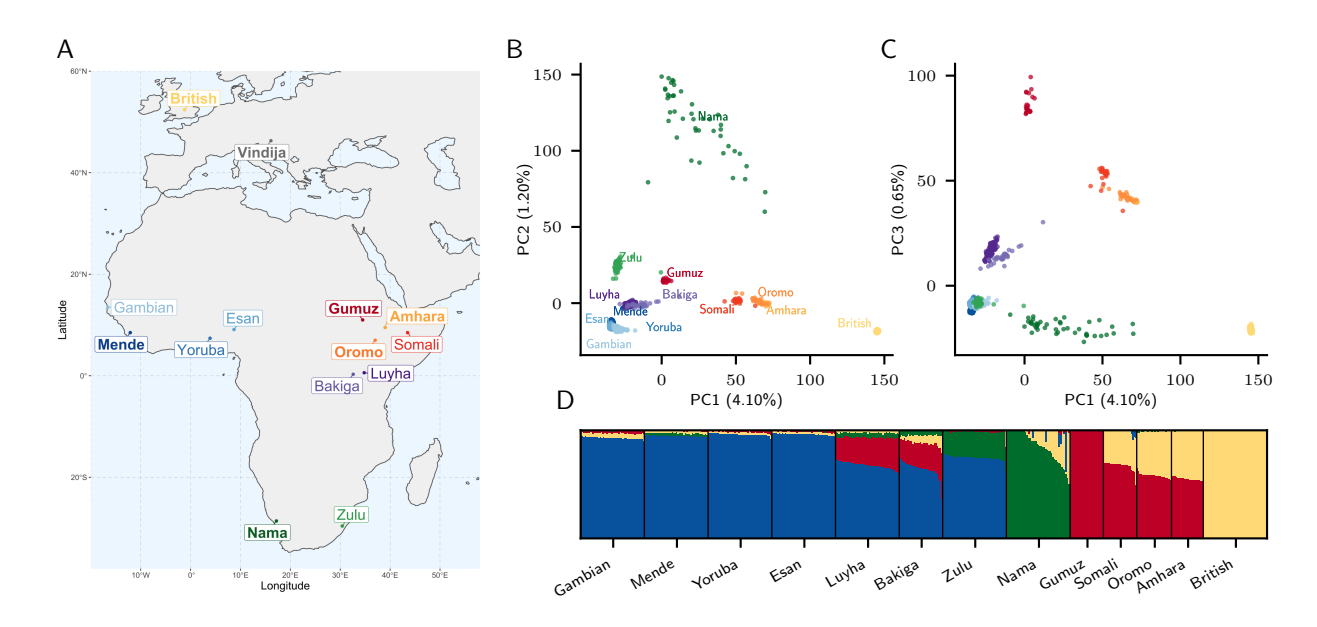


Figure 2: **Genetic diversity across Africa.** (A) Select populations from the 1000 Genomes and African Diversity Reference Panels illustrate diversity from western, eastern and southern Africa. We chose representatives from each region (bold labels) to build parameterized models, including the newly-sequenced Nama from South Africa, Mende from Sierre Leone, Gumuz, Oromo and Amhara from Ethiopia, and the British and Vindija Neanderthal individual. (B, C) PCA highlights the range of genetic divergence anchored by western Africans, Nama, Gumuz and the British. Percentages show variance explained by each principal component. (D) ADMIXTURE with K=4 illustrates signatures of recent gene flow in Africa which reflect colonial-period migration into the Nama, Back-to-Africa gene flow among some Ethiopians, and Khoe-San admixture in the Zulu.

from Neanderthals to Europeans directly following the out-of-Africa migration which was set to 1.5% at 45ka (SI Section 3.1).

We quantify migration rates among populations after their divergence  $\approx 120ka$ . Prior to agripastoralist expansion 5ka, migration between the ancestors of the Nama and other groups is an order of magnitude weaker than that observed between between western and eastern Africans (Table 1). All models infer relatively high gene flow between Ethiopia and western Africa ( $m \approx 2 \times 10^{-4}$ , the constant proportion of immigrant lineages per generation over 60ka). We further find that Back-to-Africa gene flow at the beginning of the Holocene primarily affected the ancestors of the Ethiopian agricultural populations <sup>25</sup>, comprising over half of their genetic ancestry, estimated to be 64–65%. We observe significant gene flow from the Amhara and Oromo into the Nama, a signal which is likely a proxy for the movement of eastern African caprid and cattle pastoralists <sup>26,27</sup>, here estimated to constitute a 25% ancestry contribution 2,000 ya. While this gene flow is not apparent from the ADMIXTURE plot (Figure 2), the ancestry is likely grouped into the Khoe-San component which has drifted appreciably from its ancestral eastern African source. Colonial period admixture from Europeans into the Nama was estimated at 15%, similar to proportions suggested by ADMIXTURE (Figure 2).

### Deep but connected population structure within Africa

To account for population structure prior to 135ka, three of our four models allowed for two or more "stem" populations which could diverge either before or after the Neanderthal split. We considered models both with and without migration between these stem populations, and in both cases we tested two different types of gene exchange during the expansion phase, as illustrated in Figure S7: 1) One of the stem population expands (splits into contemporary populations), and the other stem population(s) has continuous symmetric migration with those populations; or 2) one or more of the stem populations expands, with instantaneous pulse (or "merger") events from the other stem population, so that recent populations are formed by mergers



Figure 3: A weakly structured stem best describes two-locus statistics. In the two best-fitting parameterizations of early population structure, continuous migration (A) and multiple mergers (B), models that include ongoing migration between stem populations outperform those in which stem populations are isolated. Most recent populations are connected by continuous, reciprocal migration that are indicated by double-headed arrows (labels matched to migration rates and divergence times in Table 1). These migrations last for the duration of co-existence of contemporaneous populations with constant migration rates over those intervals. The merger-with-stem-migration model (B, with LL=-102,600) outperformed the continuous-migration model (A, with LL=-115,500). Colors are used to distinguish overlapping branches and link to Figure 2.

of multiple ancestral populations. Depending on parameter values, this scenario encompasses archaic hominin introgression and fragmentation-and-coalescence models (such as Figure 1B and C). For many parameters, confidence intervals based on bootstrapping are relatively narrow (Tables S3–S7), reflecting an informative statistical approach. Model assumptions have, however, a larger impact on parameter estimates (and thus, real uncertainty). To convey model uncertainty, we highlight features of the two inferred models with high likelihoods. These are referred to as the "multiple-merger" and the "continuous-migration" models. Both allow for migration between stem branches, but differ primarily in the timing of the early divergence of stem populations and their relative  $N_e$  (Figure 3). The two models also differ in the mode of divergence, with the

Likelihood	Label	Population Pair	Divergence Time (ka)	Migration rate per generation	Migration duration (kyr)
Continuous Model					
LL = -115,500	a	Stem 1, Stem 2	1,163	6.43e-5	1,028
(Table S5)	b	Stem 2, Nama	NA	5.82e-5	130
` ,	c, d	Stem 2, Other Africans*	NA	3.10e-5, <b>1.64e-4</b>	130, 55
	e, f	Nama, Other Africans*	135	4.1e-5, 9.8e-6	135, 60
	g	Mende, East Africans	60	2.14e-4	60
	$oldsymbol{\widetilde{h}}$	East Africans, British	50	4.17e-5	50
	i	Gumuz, Amhara/Oromo	12	3.36e-4	12
Merger Model		,			
LL = -102,600	a	Stem 1, Stem 2	1,442	1.16e-4	963
(Table S7)	_	Stem 1S, Stem 1E	479	0 (fixed)	_
	b	Stem 2 to Nama	119	0.71	pulse
	c	Stem 2 to Stem 1E	98	0.50	pulse
	d	Stem 2 to Mende	25	0.18	pulse
	e, f	Nama, Other Africans*	119	4.4e-5, 7.1e-6	119, 60
	g	Mende, East Africans*	60	1.98e-4	60
	$\widetilde{\mathbf{h}}$	East Africans, British	50	3.87e-5	50
	i	Gumuz, Amhara/Oromo	12	3.59e-4	12

Table 1: Migration and divergence parameters from best fit models. Labeled migration rates correspond to symmetric continuous migration bands shown in Figure 3. Both the continuous migration and merger models inferred a relatively deep split of human stem branches, though they were connected by ongoing migration that maintained their genetic similarity. Bold text indicates migration rates above  $10^{-4}$ . In both models, the branch ancestral to the Nama shares a common ancestral population with the other African groups  $\sim 120-135$ ka. Following this divergence, the population ancestral to other African groups branches into West and East African groups 60ka. \*Migration rates and durations are shown between branches ancestral to 1) Nama and East Africans and their ancestors, and 2) Nama and Mende, respectively. "Divergence times" correspond to the most recent common ancestral population, and does not account for continuous migration or earlier reticulations.

multiple-merger featuring a population reticulation during the Middle Pleistocene.

Allowing for continuous migration between the stem populations substantially improved the fits relative to zero migration between stems ( $LL \approx -102,600$  vs. -107,700 in the merger model and  $LL \approx -115,500$  vs. -126,600 in the continuous migration model). With continuous migration between stems, population structure extends back to 1.1–1.4Ma (Table 1). Migration between the stems in these models is moderate, with a fraction of migrant lineages each generation estimated as  $m = 6.4 \times 10^{-5} - 1.2 \times 10^{-4}$ . For comparison, this is similar to inferred migration rates between connected contemporary populations over the past 50ka (Table 1). This ongoing (or at least, periodic) gene flow qualitatively distinguishes these models from previously proposed archaic hominin admixture models (Figure 1C) as the early branches remain closely related, and each branch contributes large amounts to all contemporary populations (Figure 4). Because of this relatedness, only 1% to 4% of genetic differentiation among contemporary populations can be traced back to this early population structure (SI Section 5.2)

Under the continuous-migration model, one of the two stems diverges into lineages leading to contemporary populations in western, southern and eastern Africa, and the other (Stem 2) contributes variable ancestry to those populations. This migration from Stem 2 is highest with the Mende ( $m = 1.6 \times 10^{-4}$ ) compared to the Nama and East African populations ( $m = 5.8 \times 10^{-5}$  and  $3.1 \times 10^{-5}$ , respectively), with migration allowed to occur until 5ka. A sampled lineage from the Nama, Mende, and Gumuz have probabilities of being in Stem 2 at the time of Stem 1 expansion (135ka) of approximately 0.145, 0.2, and 0.13, respectively, though these probabilities change over time, precluding the notion of a fixed admixture proportion.

In contrast, under the multiple-merger model, stem populations merge with varying proportions to form the different contemporary groups. We observe a sharp bottleneck in Stem 1 down to  $N_e = 117$  after the split of the Neanderthal branch. This represents the lower bound allowed in our optimization (i.e. 1% of the ancestral  $N_e$ ), although the size of this bottleneck is poorly constrained (standard error (SE) = 838). After a long period of exchange with Stem 2, Stem 1 then fractures into "Stem 1E" and "Stem 1S" 479ka. The timing of this divergence was also poorly constrained (SE = 166ka). These populations evolve independently until 119ka (SE = 28ka) when Stem 1S and Stem 2 combine to form the ancestors of the Nama, with proportions 29%, 71% respectively. Similarly, Stem 1E and Stem 2 combine in equal proportions (50% each) to form

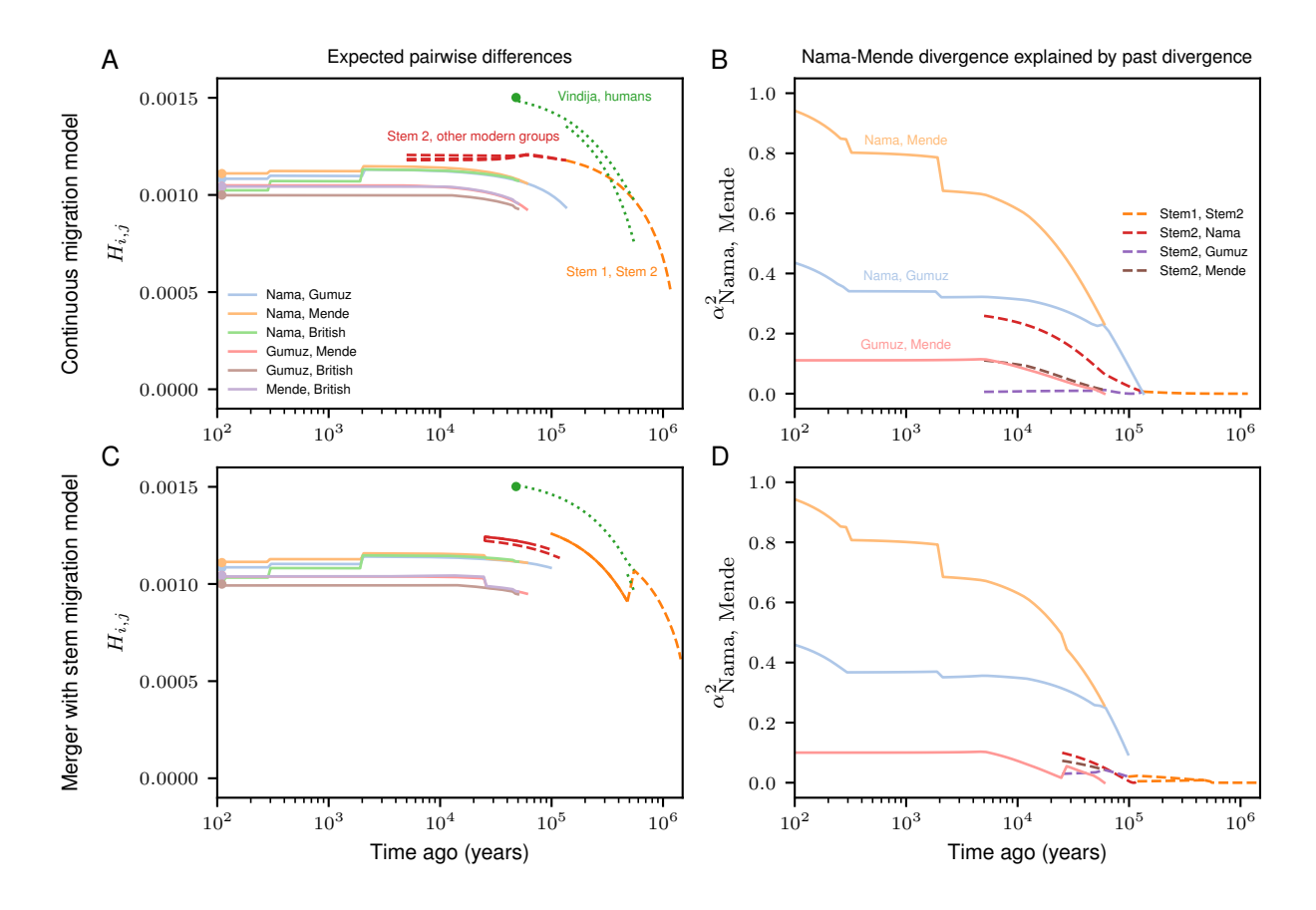


Figure 4: Structure among stems is weak and present-day structure is mostly recent. From the best fit models of our two parameterizations (A and B: continuous migration, C and D: merger with stem migration), we predicted pairwise differences  $H_{i,j}$  between individuals sampled from populations i and j existing at time t (A and C). (B and D) To understand how drift between stems explains contemporary structure, we also computed the proportion  $\alpha^2$  of drift between pairs of sampled contemporary populations that aligns with drift between past populations (here Nama and Mende, see SI Section S5.2 for details and additional comparisons in Figures S17–S20). Both models infer deep population structure with modest contributions to contemporary genetic differentiation. Most present differentiation dates back to the last 100ka.

the ancestors of the western Africans and eastern Africans (and thus also all individuals who later disperse during the Out of Africa event). Finally, the Mende receive a large additional pulse of gene flow from Stem 2, replacing 18% of their population 25ka (SE = 0.6ka). The later Stem 2 contribution to the western African Mende resulted in better model fits ( $\Delta LL \approx 60,000$ ). Speculatively, this may indicate that an ancestral Stem 2 population occupied western or central Africa, broadly speaking. The differing proportions in the Nama and eastern Africans may also indicate geographic separation of Stem 1S in southern Africa and Stem 1E in eastern Africa.

To assess robustness of the inferred models to analysis and reference population choices, SI Sections 6 and 7 present re-analyses changing the European and West African populations, as well as the recombination maps, filtering strategies and parameter optimization strategies. While we find some differences in the inferred parameters (see in particular Sections 7.1.1 and 7.2), the best fit model across all reanalyses are quantitatively consistent.

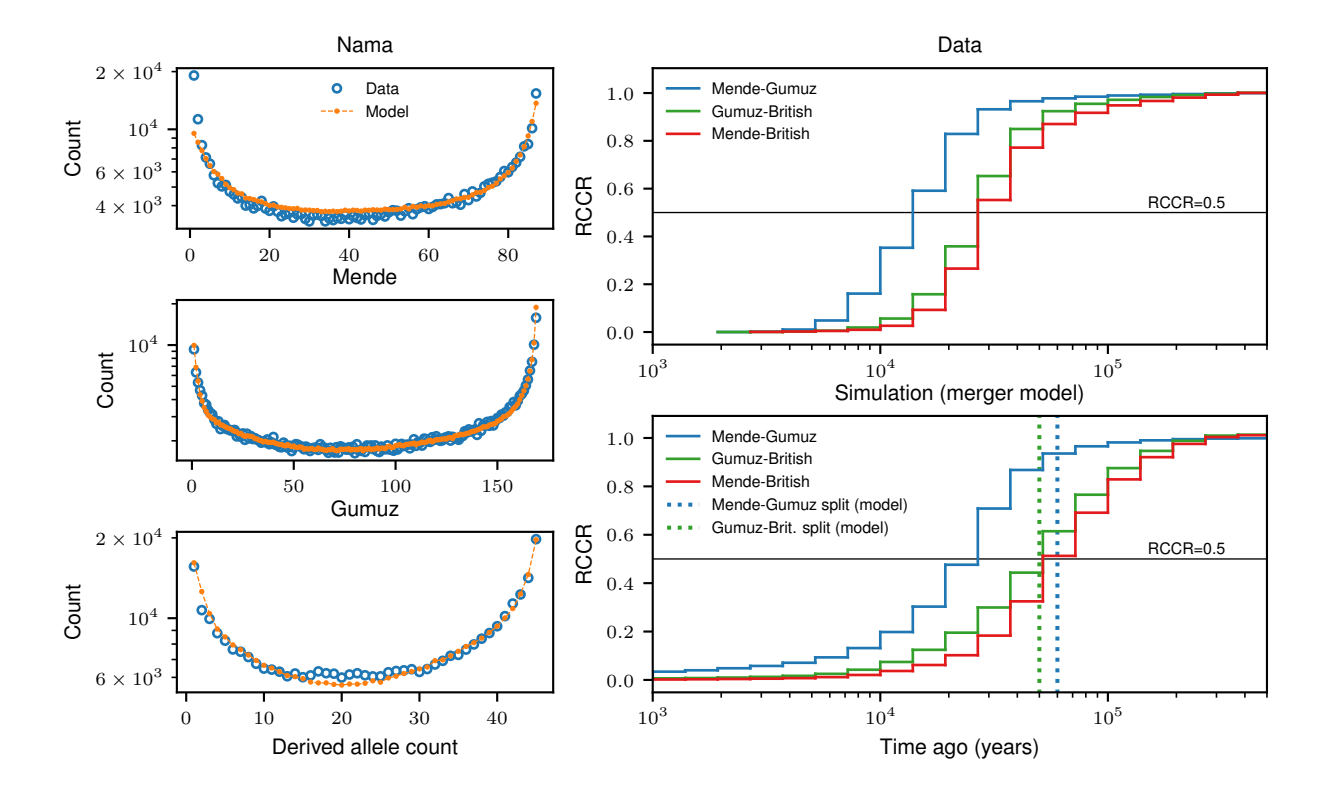


Figure 5: Model validation using independent statistics. (A–C) Using our best fit models to linkage disequilibrium and pairwise diversity statistics, we simulated expected conditional site-frequency-spectra (cSFS) and compared to the observed cSFS from the data. Our inferred models provide a good fit to the data, even though these were not used in our inference. Across the three populations, ancestral state misidentification was consistently inferred to be 1.5–1.7% for intergenic loci (SI 6.2.2). (D, E) We used Relate <sup>10</sup> to reconstruct genome-wide gene genealogies, which we used to estimate coalescence rate trajectories and cross-coalescence rates between pairs of populations. While coalescence rate distributions are informative statistics about past evolutionary processes, interpretation can be hindered by migration and population structure, and translating relative cross-coalescence rate curves (RCCR) into population divergence times is especially prone to misinterpretation. For example, the Mende-Gumuz comparison shows a more recent increased RCCR than either population with the British, a pattern that is recapitulated under our best-fit model, even though the Mende-Gumuz split occurs prior to the Gumuz-British split.

#### Reconciling multiple lines of genetic evidence

Previous studies have found support for archaic hominin admixture in Africa using two-locus statistics <sup>16,9</sup>, the conditional SFS (cSFS) <sup>15</sup>, and reconstruction of gene genealogies <sup>10</sup>. However, none of these studies considered a weakly structured stem. We validated our inferred models with additional independent approaches. We find that the observed cSFS (conditioned on the derived allele being carried in the Neanderthal sample) is very well-described by the merger model (Figures 5A-C and S21–S24), even though this statistic was not used in the fit. Our best-fit models outperform archaic hominin admixture models fit directly to the cSFS (for example, compare to Figure 1 in Durvasula and Sankararaman (2020) <sup>15</sup>). Specifically, it is the addition of migration between stems that results in a qualitative improvement of the agreement (compare Figures S23 and S24).

We used Relate<sup>10</sup> to infer the distribution of coalescence rates over time in real data and data simulated from our inferred models. Many previous studies have found a reduction of coalescence rates between 1000ka and 100ka in humans, and thus inferred an increase in  $N_e$  during the same period<sup>28</sup>. This increase in inferred  $N_e$  could be due to either an increase in population size or to ancestral population structure during the Middle Pleistocene<sup>29</sup>. All models, including the single-origin model, recapitulate an inferred ancestral increase in  $N_e$ 

between 100ka-1Ma extending deeper in the past than the Relate estimate (Figure S27 and SI Section 7.3.2). Whereas the single-origin model achieves this by an increase in  $N_e$  during that period, the best-fit model recapitulate this pattern without corresponding population size changes.

Relative cross-coalescence rates (rCCR) have recently been used to estimate divergence between a pair of populations, as measured by the rate of coalescence between two groups divided by the mean within population coalescence. Simulations of rCCR accuracy, however, focus on a 'clean split' between populations whereby groups diverge without subsequent gene flow. Published estimates of the earliest human divergences with rCCR, which range from 150ka-100ka<sup>30</sup>, may be significantly biased when compared to more complex models with gene flow as inferred here. We find that midpoint estimates of rCCR are poor estimates for population divergence, often underestimating divergence time by 50% or greater (e.g., Mende vs. Gumuz ~15ka compared to a true divergence of 60ka), and recent migration can lead to the misordering of divergence events (Figure 5E). We suggest that rCCR analyses which do not fit multiple parameters including gene flow should be interpreted with caution.

Other studies have fit tree-like demographic models to African populations using distributions of allele frequencies or related statistics, finding inconsistent divergence times, some of which are older than those we find here <sup>17,30</sup>. In the SI (Section 7.4), we show that this discrepancy can be explained by model misspecification: if divergence is estimated using an isolation with migration (IM) model with constant population sizes, but the correct model has ancient population growth or population structure, the split time in the inferred IM model is much deeper than in the correct model. Intuitively, growth or structure in the ancestral population will each increase coalescence times relative to a randomly mating population of constant size, so a model that assumes constant population sizes would require an older divergence time to fit the observed distribution of coalescence times and related statistics <sup>31,32</sup>.

### Discussion

Any attempt at building detailed models of human history is subject to model misspecification. This is true of earlier studies, which often assumed that data inconsistent with a single-origin model must be explained by archaic hominin admixture. This is also true of this study. While it remains prohibitive to fully explore the space of plausible models of early human population structure, we sought to capture model uncertainty by exploring multiple parameterizations of early history. The best fit models presented here include reticulation and migration between early human populations rather than archaic hominin admixture from long-isolated branches (Figure 1C). Elements of a recent single-origin or African multi-regionalism (Figure 1A,D) feature in our best fit models, as indicated in the recent time of contemporary population divergence or the gene flow between disparate stems, respectively. We caution that we cannot rule out that more complex models involving additional stems, continuous structure, or hybrid models including both weak structure and archaic hominin admixture may better explain the data. Because parameters related to the split time, migration rates, and relative sizes of the early stems were variable across models, reflecting a degree of confounding among these parameters, we refrained from introducing additional branches associated with more parameters during that period. Rather than interpreting the two stems as representing well-defined and stable populations over hundreds of thousands of years, we interpret the weakly structured stem as consistent with a population coalescence and fragmentation model<sup>6</sup>. Additional African populations such as those from Central Africa, other Khoe-San groups or pre-Holocene ancient DNA samples, could further test our proposed models. Given that our samples cover major ancestry components across Africa, we predict that any new admixture signal is likely to be regionally localized.

## The Formation of Population Structure in Africa

Our inferred models paint a consistent picture of the Middle to Late Pleistocene as a critical period of change, assuming that estimates from the recombination clock accurately relate to geological chronologies (SI Section 8). During the late Middle Pleistocene, the multiple merger model indicates three major stem lineages in Africa, tentatively assigned to southern (Stem 1S), eastern (Stem 1E) and western/central Africa (Stem 2). Geographic association was informed by the present population location with the greatest ancestry contribution from each stem. For example, Stem 1S contributes 71% to the ancestral formation of the Khoe-San. The extent of the isolation 400ka between Stem 1S, Stem 1E and Stem 2 suggests that these stems

were not proximate to each other. While the length of isolation among the stems is variable across fits, models with a period of divergence, isolation and then a merger event (i.e. a "reticulation") out-performed models with bifurcating divergence and continuous gene flow.

A population reticulation involves multiple stems contributing genetically to the formation of a group. One way in which this can happen is through the geographic expansion of one or both stems. For example, if during MIS 5, either Stem 1S (Figure 3B) from southern Africa moved northward thereby encountering Stem 2, or Stem 2 moved from central/western Africa southward into Stem 1S – then we could observe disproportionate ancestry contributions from different stems in contemporary groups. We observed two merger events. The first, between Stem 1S and Stem 2, results in the formation of an ancestral Khoe-San population  $\approx 120$ ka. The second event  $\approx 100$ ka between Stem 1E and Stem 2, results in the formation of the ancestors of Eastern/Western Africans including the ancestors of "Out of Africans". The rapid rise in sea levels and increased precipitation during MIS 5e interglacial, following a glacial period of aridity across Africa 33, might have triggered migration inland away from the coasts, as has been suggested, e.g., for the Paleo-Agulhas plain  $^{34}$ .

Following these merger events, the stems subsequently fracture into subpopulations which then persist over the past  $\sim 120 \mathrm{ka}$ . These subpopulations can be linked to contemporary groups despite subsequent gene flow across the continent; for example, a genetic lineage sampled in the Gumuz has a 0.44 probability of being inherited from the ancestral 'eastern' subpopulation (Stem 1E) 150ka versus 0.03 probability of being inherited from the 'southern' subpopulation (Stem 1S) and 0.53 probability of being inherited from Stem 2 (see Table S9 for additional comparisons). We also find that Stem 2 continued to contribute to western Africans during the Last Glacial Period, indicative that this gene flow likely occurred in western/central Africa (Table 1). Such an interpretation is reinforced by the differential migration rates between regions, i.e. the gene flow from Stem 2 to western Africans is 5x that of the rate to eastern Africans during this period. We performed a variety of validation tests to explore sensitivity of our assumptions, including relaxing fixed parameters (SI Section 6). Most validation tests resulted in parameters similar to the models discussed above. However, one exception was the inferred Out of Africa and Eastern/Western divergence which were 10-15ka younger than our fixed parameters. Complexity of this event warrants additional Eurasian populations and greater detail; nonetheless, our model mis-specification of this event does not change other features of the merger model.

### Contrasting archaic hominin admixture and a weakly structured stem

Evidence for archaic hominin admixture in Eurasia has bolstered the plausibility of archaic hominin admixture having also occurred in Africa. Previous work that sought to explain patterns of polymorphism inconsistent with a single-origin model thus focused on archaic hominin admixture as an alternative model. The additional (or "ghost") branches required to fit the data are systematically referred to as "archaic" <sup>11,12,13,9,14,15</sup>, and assumed (or inferred) to be deeply diverged. We believe that this has strongly oriented the interpretation of these results (e.g., regarding selection <sup>35</sup> or the fossil record?). Here, we have shown that weakly-structured-stem models better captures the apparently inconsistent patterns of polymorphisms. Preferring weakly-structured-stem models over archaic-admixture models potentially has a range of implications.

First, with a weakly structured stem, there is no need to posit that an archaic hominin population in Africa stayed reproductively isolated from the ancestral human lineage for tens thousands of years before the initiation of gene flow. Instead, there would simply have been continuous or recurrent contact between two or more groups present in Africa.

Second, there is evidence for both deleterious and adaptive archaic-hominin-derived alleles in contemporary genomes in the form of a depletion of Neanderthal ancestry in regulatory regions <sup>36</sup> or an increased frequency of archaic-hominin-related haplotypes such as at *EPAS1* among Tibetans <sup>37</sup>. Under previous African archaic hominin admixture models, the estimated 8–10% introgression rate is much higher than Neanderthal gene flow, and would have plausibly been fertile ground for dramatic selection for or against archaic-hominin-derived haplotypes <sup>35</sup>. By contrast, adaptation under a weakly structured stem would have occurred continuously over much longer periods. Patterns of polymorphism that are inconsistent with the single-stem model predictions have been used to infer putative archaic admixed segments <sup>11,16,35,15</sup>, negative selection against such segments <sup>35</sup>, and pervasive positive selection <sup>38</sup>. However, such approaches are subject to high false positives in the presence of population structure with migration <sup>36</sup>, and their interpretation

should be re-examined in light of a weakly-structured-stem model within Africa.

Third, multiple studies have shown a correspondence between phenotypic differentiation, usually assessed with measurements of the cranium, and genetic differentiation among human populations and between humans and Neanderthals <sup>39,40,41</sup> (see also SI Section 5.4). This correspondence potentially allows predictions of our model to be related to the fossil record. The fossil record of Africa is sparse during the time period of the stems, but of the fossils that date to this time period, some are fairly similar in morphology to contemporary humans (e.g., Omo 1 from Omo Kibish, Ethiopia <sup>42,43</sup>), others are similar in some morphological features to contemporary humans (e.g., Irhoud 1 from Jebel Irhoud, Morocco <sup>1,44</sup>), and others are different enough in morphology to have been assigned to species other than *Homo sapiens* (e.g., DH1 from Dinaledi, South Africa <sup>45,46</sup>). If, as our model predicts, the genetic differences between the stems were comparable to those among contemporary human populations, the most morphologically divergent fossils are unlikely to represent branches that contributed appreciably to contemporary human ancestries.

## 315 Data availability

304

305

307

308

309

310

311

312

313

314

All sequencing data are available from XXX, accession number: YYY.

## 317 Code availability

```
Code for the software used in this paper is found at the following locations:
moments-LD (https://bitbucket.org/simongravel/moments),
Demes (https://github.com/popsim-consortium/demes-python),
Relate (https://myersgroup.github.io/relate/),
msprime (https://github.com/tskit-dev/msprime),
tskit (https://github.com/tskit-dev/tskit),
and scripts implementing analyses using each of these software are available at
https://github.com/apragsdale/african-structure-paper.
```

# $_{\scriptscriptstyle{326}}$ Acknowledgements

We are grateful for the DNA contribution from each participant which enabled this study; in particular we 327 wish to highlight the generous participation of the Richtersveld Nama community in South Africa and help 328 329 from local research assistants Willem DeKlerk and Hendrik Kaimann. Additional assistance and community engagement was conducted by Justin Myrick, Chris Gignoux, Caitlen Uren and Cedric Werely. We thank 330 the African Genome Diversity Project for data generation, including Tommy Carensten, Deepti Gurdasani, 331 and Manj Sandhu. We thank Luke Anderson-Trocmé and Georgette Femerling for assistance in creating the 332 map in Figure 2 and Figure S2, respectively. This research was supported by an NIH grant R35GM133531 333 (to BMH). The content is solely the responsibility of the authors and does not necessarily represent the 334 official views of the National Institutes of Health. 335

#### 6 References

- [1] Hublin, J.-J. *et al.* New fossils from Jebel Irhoud, Morocco and the pan-African origin of Homo sapiens.

  Nature **546**, 289–292 (2017).
- <sup>339</sup> [2] White, T. D. *et al.* Pleistocene Homo sapiens from Middle Awash, Ethiopia. *Nature* **423**, 742–747 (2003).
- [3] Deacon, H. J. Two Late Pleistocene-Holocene Archaeological Depositories from the Southern Cape,
   South Africa. The South African Archaeological Bulletin 50, 121–131 (1995).
- [4] Stringer, C. The origin and evolution of Homo sapiens. *Philos. Trans. R. Soc. Lond. B Biol. Sci.* **371** (2016).

- [5] Scerri, E. M. L. et al. Did Our Species Evolve in Subdivided Populations across Africa, and Why Does
   It Matter? Trends Ecol. Evol. 33, 582-594 (2018).
- [6] Scerri, E. M. L., Chikhi, L. & Thomas, M. G. Beyond multiregional and simple out-of-Africa models of human evolution. Nat Ecol Evol 3, 1370–1372 (2019).
- <sup>349</sup> [7] Arredondo, A. *et al.* Inferring number of populations and changes in connectivity under the n-island model. *Heredity* **126**, 896–912 (2021).
- <sup>351</sup> [8] Kamm, J., Terhorst, J., Durbin, R. & Song, Y. S. Efficiently inferring the demographic history of many populations with allele count data. *J. Am. Stat. Assoc.* **115**, 1472–1487 (2020).
- <sup>353</sup> [9] Ragsdale, A. P. & Gravel, S. Models of archaic admixture and recent history from two-locus statistics. PLoS Genet. **15**, e1008204 (2019).
- <sup>355</sup> [10] Speidel, L., Forest, M., Shi, S. & Myers, S. R. A method for genome-wide genealogy estimation for thousands of samples. *Nat. Genet.* **51**, 1321–1329 (2019).
- <sup>357</sup> [11] Plagnol, V. & Wall, J. D. Possible ancestral structure in human populations. *PLoS Genet.* **2**, e105 (2006).
- [12] Hammer, M. F., Woerner, A. E., Mendez, F. L., Watkins, J. C. & Wall, J. D. Genetic evidence for archaic admixture in Africa. Proc. Natl. Acad. Sci. U. S. A. 108, 15123-15128 (2011).
- [13] Hey, J. et al. Phylogeny Estimation by Integration over Isolation with Migration Models. Mol. Biol. Evol. 35, 2805–2818 (2018).
- <sup>363</sup> [14] Lorente-Galdos, B. *et al.* Whole-genome sequence analysis of a Pan African set of samples reveals archaic gene flow from an extinct basal population of modern humans into sub-Saharan populations. *Genome Biol.* **20**, 77 (2019).
- Durvasula, A. & Sankararaman, S. Recovering signals of ghost archaic introgression in African populations. Sci Adv 6, eaax5097 (2020).
- <sup>368</sup> [16] Hsieh, P. *et al.* Model-based analyses of whole-genome data reveal a complex evolutionary history involving archaic introgression in Central African Pygmies. *Genome Res.* **26**, 291–300 (2016).
- <sup>370</sup> [17] Henn, B. M., Steele, T. E. & Weaver, T. D. Clarifying distinct models of modern human origins in Africa. *Curr. Opin. Genet. Dev.* **53**, 148–156 (2018).
- <sup>372</sup> [18] Lipson, M. *et al.* Ancient DNA and deep population structure in sub-Saharan African foragers. *Nature* **603**, 290–296 (2022).
- <sup>374</sup> [19] 1000 Genomes Project Consortium *et al.* A global reference for human genetic variation. *Nature* **526**, 68–74 (2015).
- <sup>376</sup> [20] Gurdasani, D. *et al.* The African Genome Variation Project shapes medical genetics in Africa. *Nature* 517, 327–332 (2015).
- <sup>378</sup> [21] Gopalan, S. *et al.* Hunter-gatherer genomes reveal diverse demographic trajectories during the rise of farming in Eastern Africa. *Curr. Biol.* **32**, 1852–1860.e5 (2022).
- Pagani, L. et al. Tracing the route of modern humans out of Africa by using 225 human genome sequences from Ethiopians and Egyptians. Am. J. Hum. Genet. 96, 986–991 (2015).
- <sup>382</sup> [23] Prüfer, K. *et al.* A high-coverage Neandertal genome from Vindija Cave in Croatia. *Science* **358**, 655–658 (2017).
- <sup>384</sup> [24] Ragsdale, A. P. & Gravel, S. Unbiased Estimation of Linkage Disequilibrium from Unphased Data. <sup>385</sup> Mol. Biol. Evol. **37**, 923–932 (2020).

- <sup>386</sup> [25] Molinaro, L. *et al.* West Asian sources of the Eurasian component in Ethiopians: a reassessment. *Sci.*<sup>387</sup> *Rep.* **9**, 18811 (2019).
- <sup>388</sup> [26] Henn, B. M. *et al.* Y-chromosomal evidence of a pastoralist migration through Tanzania to southern Africa. *Proc. Natl. Acad. Sci. U. S. A.* **105**, 10693–10698 (2008).
- <sup>390</sup> [27] Breton, G. *et al.* Lactase persistence alleles reveal partial East African ancestry of southern African Khoe pastoralists. *Curr. Biol.* **24**, 852–858 (2014).
- <sup>392</sup> [28] Li, H. & Durbin, R. Inference of human population history from individual whole-genome sequences.

  Nature 475, 493–496 (2011).
- [29] Mazet, O., Rodríguez, W., Grusea, S., Boitard, S. & Chikhi, L. On the importance of being structured:
   instantaneous coalescence rates and human evolution—lessons for ancestral population size inference?
   Heredity 116, 362–371 (2016).
- <sup>397</sup> [30] Bergström, A., Stringer, C., Hajdinjak, M., Scerri, E. M. L. & Skoglund, P. Origins of modern human ancestry. *Nature* **590**, 229–237 (2021).
- [31] Momigliano, P., Florin, A.-B. & Merilä, J. Biases in Demographic Modeling Affect Our Understanding of Recent Divergence. Mol. Biol. Evol. 38, 2967–2985 (2021).
- [32] Shchur, V., Brandt, D. Y. C., Ilina, A. & Nielsen, R. Estimating population split times and migration rates from historical effective population sizes. *bioRxiv* 2022.06.17.496540 (2022).
- Blome, M. W., Cohen, A. S., Tryon, C. A., Brooks, A. S. & Russell, J. The environmental context for the origins of modern human diversity: A synthesis of regional variability in African climate 150,000–30,000 years ago. J. Hum. Evol. 62, 563–592 (2012).
- <sup>406</sup> [34] Marean, C. W. *et al.* Stone Age people in a changing South African Greater Cape Floristic Region. In *Fynbos* (Oxford University Press, 2014).
- Wall, J. D., Ratan, A., Stawiski, E. & GenomeAsia 100K Consortium. Identification of African-Specific Admixture between Modern and Archaic Humans. Am. J. Hum. Genet. 105, 1254–1261 (2019).
- [36] Petr, M., Pääbo, S., Kelso, J. & Vernot, B. Limits of long-term selection against Neandertal introgression. *Proc. Natl. Acad. Sci. U. S. A.* **116**, 1639–1644 (2019).
- [37] Zhang, X. et al. The history and evolution of the Denisovan-EPAS1 haplotype in Tibetans. Proc. Natl. Acad. Sci. U. S. A. 118 (2021).
- [38] Schrider, D. R. & Kern, A. D. Soft Sweeps Are the Dominant Mode of Adaptation in the Human Genome. Mol. Biol. Evol. 34, 1863–1877 (2017).
- [39] Relethford, J. H. Craniometric variation among modern human populations. Am. J. Phys. Anthropol. 95, 53–62 (1994).
- 418 [40] Weaver, T. D., Roseman, C. C. & Stringer, C. B. Close correspondence between quantitative- and molecular-genetic divergence times for Neandertals and modern humans. *Proc. Natl. Acad. Sci. U. S.*420 A. **105**, 4645–4649 (2008).
- [41] von Cramon-Taubadel, N. Congruence of individual cranial bone morphology and neutral molecular affinity patterns in modern humans. Am. J. Phys. Anthropol. 140, 205–215 (2009).
- 423 [42] Day, M. H. Omo human skeletal remains. Nature 222, 1135–1138 (1969).
- <sup>424</sup> [43] Vidal, C. M. *et al.* Age of the oldest known Homo sapiens from eastern Africa. *Nature* **601**, 579–583 (2022).
- <sup>426</sup> [44] Richter, D. *et al.* The age of the hominin fossils from Jebel Irhoud, Morocco, and the origins of the Middle Stone Age. *Nature* **546**, 293–296 (2017).

- <sup>428</sup> [45] Berger, L. R. *et al.* Homo naledi, a new species of the genus Homo from the Dinaledi Chamber, South Africa. *Elife* 4 (2015).
- <sup>430</sup> [46] Dirks, P. H. *et al.* The age of Homo naledi and associated sediments in the Rising Star Cave, South Africa. *Elife* **6** (2017).